Research Square

Preprints are preliminary reports that have not undergone peer review.
They should not be considered conclusive, used to inform clinical practice,
or referenced by the media as validated information.

Characterization of selected station sites of the Hellenic Accelerometer Network (HAN)

Nikolaos Theodoulidis
ntheo@itsak.gr

Inst. Engineering Seismology and Earthquake Engineering https://orcid.org/0000-0002-0169-9197
Fabrice Hollender
CEA Cadarache Centre: Commissariat a l'energie atomique et aux energies alternatives Centre de Cadarache
Pauline Rischette
CEA Cadarache Centre: Commissariat a l'energie atomique et aux energies alternatives Centre de Cadarache
Ioannis Grendas
Inst. Engineering Seismology and Earthquake Engineering
Zafeiria Roumelioti
University of Patras, Department of Geoiogy
Hussein Shible
BRGM: Bureau de Recherches Geologiques et Minieres

Research Article

Keywords: Site Characterization, Accelerometer Stations, Engineering Reference Site, Ambient Noise Array & MASW geophysical methods

Posted Date: May 7th, 2026

DOI: https://doi.org/10.21203/rs.3.rs-9370620/v1

License: This work is licensed under a Creative Commons Attribution 4.0 International License. Read Full License

Abstract

Abstact

In this study site characterization of twelve accelerometer station sites of the Hellenic Accelerometers Network (HAN) is presented. An established European protocol is applied that consists of non-invasive active (Multichannel Analysis of Surface Waves: MASW) and passive (Ambient Vibration Analysis: AVA) methods. Data processing is carried out systematically, using new techniques of dispersion curves estimation and their inversion to obtain 1D shear wave velocity profiles at the examined sites. Surface geology and other site information previously indicated six sites as reference “rock” and six as stiff to soft soil. After data processing in this study, it was determined that only five of them fulfil the engineering bedrock criterion (V_{S30} > 800 m/s), with one of them - station ART2 (Arta) - identified as very hard rock (V_{S30} ~2000 m/s). The remaining seven investigated sites fall within stiff to soft soil categories (380 ≤ V_{S30} ≤ 618 m/s). The results show that, for stiff soil and rock sites, geology and topographic slope- inferred V_{S30} values, in some cases significantly, especially for V_{S30} > 500 m/s. These results highlight the importance of direct geophysical investigation for reliable site classification and for reducing bias in ground motion modeling, e.g. Ground-Motion Models (GMMs) and Generalized Inversion Techniques (GITs). The updated station sites characterization metadata set provides a reference framework for future updates of the Hellenic Accelerometers Network recordings and contributes to the harmonization of European strong-motion stations metadata within EPOS as well as in the European Strong Motion database.

1 Introduction

Site characterization is an important component in assessing seismic hazard, usually incorporating *in situ* shear wave velocity as a function of depth ($V_S\,(z)$), as well as the estimation of site amplification and the fundamental frequency of the site (f_0). All site characteristics are captured by the ground motion recordings and depend on several geophysical parameters that characterize surficial geological layers with thickness of several up to few hundred meters. Site characterization of accelerometer stations is of high importance since its information can contribute to the full and efficient use of accelerogram recordings. Accelerogram databases usually provide such data and metadata for robustly defining Ground Motion Models (GMMs), as well as for Generalized Inversion Techniques (GITs) applications, which are used in seismic hazard assessment. However, it is known that accelerometer recordings on reference rock sites, that is, recording sites free of site effects, are limited worldwide compared to other soil types (e.g. soft rock, stiff or soft soils). Consequently, proposed GMMs are generally not well constrained for reference rock ground-motion prediction, and they better represent soft and stiff soils. In addition, application of GIT may lead to improved results when recordings on reference rock sites and associated data is included in the dataset to constrain inversions (e.g. Nakano et al. 2015; Shible et al. 2022; Grendas et al. 2022; Shible et al. 2023a).

Site characterization can be performed by invasive or non-invasive techniques. Non-invasive geophysical methods offer an affordable alternative for acquiring a V_S profile using body or surface wave techniques at the surface of the investigated site contrary to invasive methods that require drilling of a borehole (Garofalo et al. 2016; Foti et al. 2018). Non-invasive methods can be differentiated into active-source array methods (e.g. multichannel analysis of surface waves: MASW) and passive-source array methods (e.g. Ambient Vibration Array: AVA).

The definition of a reference rock site is a debatable issue (e.g. Steidl et al. 1996). To this direction quantitative measures have been proposed based mainly on shear wave velocity of the uppermost geologic layers. One of them refers to the time-averaged shear wave velocity in the uppermost 30 m of the examined site, the well-known V_{S30} value introduced (Borcherdt 1994). This measure has been adopted by many seismic codes worldwide among which is the Eurocode 8: EC8 (CEN 2004), by considering a site as a reference rock when V_{S30} is equal or greater than 800 m/s. Due to limitations/constrains of this parameter in estimating site amplification in a broad range of frequencies, another parameter has recently been introduced that is defined by the bedrock depth at which V_S is equal or greater than 800 m/s, known as H_{800}, the so-called engineering bedrock (e.g. Cultrera et al. 2021; Di Giulio et al. 2012). This parameter along with the site fundamental frequency (f_0) proved to be more informative than V_{S30} alone. Since the amplification of ground motion can start at the seismic bedrock level where the shear wave velocity reaches approximately 3 km/s, generic amplification factors have been proposed (e.g., Boore and Joyner 1997; Margaris and Boore 1998). Consequently, the shear wave velocity profile up to that depth though hard to measure, could be very useful for rational estimation of site amplification.

Characterizing sites of seismic stations has now become essential, especially for strong motion databases, since recordings are shaped by their substructure dynamic properties ($V_S\,(z)$, $V_p\,(z)$, ρ etc.) the well-known site effects. During the past two decades many efforts have been made towards station site characterization worldwide (in Japan Kik-NET: https://www.kyoshin.bosai.go.jp/kyoshin/docs/overview_kyoshin_index_en.html; in USA: Yong et al. 2013; in New Zealand: Van Houtte et al. 2012; in S. Korea: Lee et al, 2025; among others) as well as in Europe (Foti et al. 2011; Hollender et al. 2018; Lanzano et al. 2021; Pilz et al. 2020; among others).

In Greece the first effort for station site characterization (Theodoulidis and Papazachos 1992) was based on geology and mechanical characteristics of surface soil layers, ranking them in three rough categories, namely, “rock”, “stiff” and “soft” soil formations. Over time, especially in the last 15 years, sporadic measurements (e.g. Cross hole, Down hole, Ambient Vibration Arrays) have been performed at some station sites. Results of these efforts have been included in Stewart et al. (2014) along with inferred V_{S30} values based on a combination of proxies including the surface geology, the topographic slope and the terrain category. Later, Margaris et al. (2021) provided a flat file of ground motion intensity measures in Greece together with their metadata, including site characterization parameters in terms of surface geology and V_{S30} values, for more than 330 accelerometer stations in Greece. However, only about 20% of them have been characterized by in-situ geotechnical or/and geophysical methods (invasive or/and non-invasive) performed at a distance $\leq$ 100 m from the station while most of the stations were characterized by proxy inferred V_{S30} values and no analytical $V_S\,(z)$ profile was given. In addition, regarding “rock” reference stations with V_{S30} values equal or greater than 800 m/s, very few of them (< 5) have been characterized till now, showing V_{S30} values ranging between 839 $\leq$ V_{S30} $\leq$ 1183 m/s (Margaris et al. 2021). Papadopoulos et al. (2023) conducted site characterization at six accelerometer station sites in the metropolitan area of Thessaloniki using surface wave methods along with the electrical resistivity technique.

Recently, Ktenidou et al. (2026), questing reference stations in Greece, presented a methodology for site characterization of sixty seismic stations owned by the Geodynamic Institute of the National Observatory of Athens. Their approach was based on several criteria, including mainly Horizontal-to-Vertical Spectral ratios (HVSRs) of earthquake recordings along with several other proxies (e.g. geology, slope, installation conditions), derived from existing datasets and metadata, without additional field measurements. By compiling all descriptors and derived amplification characteristics from strong motion data, they co-evaluated the overall potential of the examined sites as reference stations. No numerical values were attributed to each presented parameter, but they opted to assess all data together to show an overall qualitative assessment, resulting in five preferred rock reference stations.

From the above it follows that the number of accelerometer station sites in Greece assigned quantitative characterization (e.g. V_{S30}, $V_S(z)$, Vsp-profiles, depth to bedrock) based on in situ geophysical measurements remains limited, especially regarding the "rock" reference sites. In this study combined noninvasive passive and active geophysical techniques are applied at twelve accelerometer station sites in Greece, following a standardized procedure (Hollender et al. 2018) to provide a quantitative, measurement-based and uncertainty-included improvement for earthquake site characterization within the Hellenic Accelerometer Network (HAN). The analysis focuses on six stations installed on geologic "rock" and six on stiff to soft soil conditions. Determination of $V_S(z)$ 1D-profiles down to the seismological bedrock depth ($V_S \geq$ 3 km/s), as well as of V_{S30} and H_{800} values and site class according to EC8, is pursued. To form a holistic picture of site characterization, surface geology is also provided for the examined stations. The results of this study aim at contributing to the improvement of GIT determined parameters (of source, path, site) and the accuracy of GMMs for "rock" site conditions.

2 SELECTION OF STATION SITES

2.1 reference "Rock" station sites

To establish GMMs specific to very hard rock conditions and adapted to the Euro-Mediterranean context a fundamental study has been conducted by Shible et al. (2026). This approach was based on deconvolving accelerograms using GIT results. This method, initially developed using Japanese data (Shible et al. 2023a; Shible et al. 2023b), requires the identification of reference stations with the lowest possible site effects for which S-wave velocity profiles are available.

While such information already existed for station sites in several European countries (France, Italy, Switzerland, etc.), this was not the case for Greece, even though this country provides a significant portion of the European accelerogram records. We were, therefore, motivated to identify accelerometer station sites in Greece that could serve as reference, and then to characterize them during a field campaign which was conducted in November 2023. We describe hereafter the process that led to the pre-selection of the six potential reference stations.

The accelerometric network in Greece (Hellenic Accelerometer Network, HAN) has been developed over the past 50 years in various deployment periods with different types of accelerometers, spanning from the analog era to the digital and the broadband digital. The primary network operators in Greece are the Institute of Engineering Seismology & Earthquake Engineering (ITSAK) and the Geodynamic Institute of the National Observatory of Athens (GEIN-NOA). The main milestones toward the development of HAN have been, (i) the establishment of ITSAK in early 1980s when the first planning and deployment of the HAN was implemented with installation of 50 analog type accelerometers throughout Greece (Theodoulidis et al. 1986), and (ii) the later update and extension of the network by ITSAK and GEIN-NOA with about 200 broadband digital accelerometers. Today HAN counts more than 300 active accelerometer stations. Details about the evolution of the HAN can be found in Margaris et al. (2014).

Best practices in site characterization include the determination of the full $V_S(z)$ profiles down to rock, mainly based on geophysical investigation. Regarding site characterization of the HAN stations in terms of V_{S30} values, for the vast majority (~ 80%) an inferred V_{S30} value has been attributed, rather than a measured one. Most such inferred values have been based on the surface geology and the gradient slope-proxy as has been proposed by Stewart et al., (2014). Such an approach is recommended compared to the gradient-only approach of Wald and Allen, (2007). For the rest ~ 20% of the stations a measured V_{S30} is allocated within a 'geophysical measurement-to-station' distance less than 100 m. However, even in this 20% there are only very few "rock" reference stations ($V_{S30} \geq$ 800m/s) of HAN. Consequently, "rock" reference stations have been mainly characterized based either on inferred values or on a qualitative surface geology description (EAGME geological maps, scale 1:500 000 https://www.eagme.gr/).

Only recently, Horizontal Spectral Amplification Factors (HSAFs) as well as HVSRs have been proposed for stations of the HAN based on the Generalized Inversion Technique (GIT), as well as on HVSR of S-waves (Grendas et al. 2021; Maragkakis 2022; Theodoulidis et al. 2022). We used these previously proposed HSAFs and HVSRs in combination with certain criteria with respect to their averaged values and standard deviation over selected frequency ranges. These criteria, along with the reasoning for the examined frequency ranges, are listed in Table 1. The criteria refer to:

The lowest standard deviation in $\log_{10}$, i.e., mostly flat amplification over the selected frequency range.

The lowest average response (over the selected frequency range), i.e., the lowest level or amplification values.

Following the application of the criteria in Table 1, a list of 17 stations was obtained, which are located throughout Greece (Fig. 1).

Table 1
Criteria applied to previously proposed HSAF and HVSR for HAN stations (see text for references) for the selection of candidate rock-reference stations identified as those with the lowest on average amplification and standard deviation. Stations that fulfil the set criteria are listed in the last column.

No.	Criteria	Function	Frequency Range [Hz]	Consequence	List of stations
1	Lowest average & standard deviation	HSAF (1)	0.3–15	Allows selection of low amplification stations (almost flat response) and standard deviation in a broad frequency range	SEIS, ART2, NAX1, AIG2, KYP2, VSK1
2	Lowest average & standard deviation	HSAF	0.3-8.0	Allows to avoid high-frequency effects and GIT trade-offs	SEIS, ART2, VSK1, PAT5, AST1, ATH5, AIG2
3	Lowest average	HSAF	0.3-1.0	Allows to avoid stations with deep basin sediments, where 1D simulations can be insufficient. Possible Amplification will be due to shallow layers.	SEIS, NAX1, STL1, ART2, RLN1, LMS2, SIA1
4	Lowest std	HVSR (2)	0.3-8.0	Can contribute to selecting stations with flat response.	SIA1, SEIS, FRS1, TRP1, ART2, LEO1, PIR1

(1) HSAF: Horizontal Site Amplification Function.

(2) HVSR: Horizontal-to-Vertical Spectral Ratio.

In Table 2 the selected 17 stations are sorted according to the number of criteria they satisfy and the number of available strong motion records in the employed dataset. The latter spans the period 1973–2018. All candidate “rock” stations have recorded > 30 strong motion records, i.e., a sufficient number in the statistical sense. Among the 17 stations, it was finally decided to keep as candidate “rock” reference stations for characterizations, only those satisfying at least 2 out of 4 initial selection criteria, that is 6 accelerometer stations. An exception was made for station NAX1 located on the island of Naxos, that was excluded from the list due to logistic reasons (e.g., costly access and implementation of afield campaign). However, it was replaced by station ATH5, which although satisfies only one criterion, it is of high importance due to its location in the capital of Greece, Athens, where more than 10 stations are installed in a variety of soil conditions, and it is housed in the building of National Parliament. Station AST1 satisfying also one criterion but it is excluded because its location is close enough to the VSK1 station.

Table 2
Sorted list - according to the number of satisfied selection criteria and available strong motion records - of the17 stations examined as candidate “rock” sites for site characterization.

No.	Station Code	Latitude	Longitude	Number of satisfied criteria	Number of records in database (1973–2018)
1	ART2	39.1474	20.99368	4	100
2	SEIS	40.6318	22.9628	4	69
3	AIG2	38.2417	22.0726	2	99
4	NAX1	37.1014	25.3741	2	98
5	SIA1	40.2573	21.5534	2	90
6	VSK1	38.4091	20.5640	2	85
7	AST1	38.5416	21.0895	1	124
8	ATH5	37.9754	23.7371	1	39
9	FRS1	39.2934	22.3844	1	101
10	KYP2	37.2497	21.6670	1	84
11	LMS2	40.8349	21.1418	1	68
12	PAT5	38.2959	21.7951	1	84
13	PIR1	37.9372	23.6426	1	84
14	RLN1	36.0891	28.0869	1	56
15	STL1	40.6624	22.9353	1	42
16	TRP1	37.5112	22.3634	1	99
17	LEO1	37.1689	22.8637	1	93

Finally, the selected potential “rock” reference stations for site characterization are the ART2 (Arta), SEIS (Thessaloniki), AIG2 (Aigion), SIA1 (Siatista), VSK1 (Vasilikiades), and ATH5 (Athens). Their HSAF, VSAF and earthquake HVSR are shown in Fig. 2 (Maragkakis, 2022).

2.2 Stiff and soft station sites

The selection of the rest six stiff and soft soil station sites was based on the framework of a parallel project regarding the effect of buildings on strong motion recordings, which involved measurements carried out inside and close to the buildings (Rischette et al., 2026). This project required accurate characterization of the under-study sites and motivated us to include them as target sites of the present study, as well. These station sites are the ARG2 (Argostoli), LEF2 (Lefkas), PLA1 (Thessaloniki), ITS1 (Thessaloniki), JAN2 (Ioannina), and LXR2 (Lixouri) (Fig. 1). Their HSAF, VSAF and earthquake HVSR are shown in Fig. 2 (after Maragakis, 2022). Surface geology, based on geological maps around the selected six stiff and/or soft soil stations are presented in Fig. 3.

3 METHODS AND DATA used

During the past two decades, site characterization using non-invasive methods based on the measurement of surface wave dispersion feature to obtain a $V_S\,(z)$ profile by inversion, is constantly gaining ground worldwide (Foti et al. 2018; Yong et al. 2022). The methodology used to characterize the twelve selected Greek stations is the same one that was developed and implemented for the characterization of French stations within the Epos-France framework and detailed in Hollender et al. (2018). We use the active MASW method to characterize the uppermost superficial layers (up to ~ 10 m) and the passive AVA method for investigating larger depth (up to several hundred meters in the geometries we implement), following the recommendations set out in the InterPACIFIC guidelines (Foti et al. 2018).

3.1 Multichannel Analysis of Surface Waves (MASW) and Acquisition Layout

The MASW method (Park et al. 1999) investigates the dispersion of surface waves (Rayleigh or/and Love waves) to generate a 1D S-wave velocity ($V_S\,(z)$) profile. It deserves mentioning that during the generation of surface waves with a compressional source, more than $2/3$ of the total seismic energy is carried by Rayleigh waves (Richart et al., 1970). In heterogenous media, such as the shallow layers of the Earth, Rayleigh wave velocity varies with depth, and different frequency bands of Rayleigh waves propagate at different phase velocities. Consequently, different wavelengths exist for each frequency, and this phenomenon is called dispersion. Dispersion of surface waves is utilized to study the elastic properties of surface geological formations (Nazarian et al., 1983; Park et al., 1998; Stokoe et al., 1994). Dispersion mainly depends on V_S in geological formations. More details about the applicability and limitations of the active MASW method can be found, among others, in Foti et al., (2018).

The acquisition layout includes a linear array of receivers with the shot position in-line with the receivers. The geometry is defined by the array length L, the receiver spacing Δx, and the source distance from the receivers. The nominal measurement protocol that we adopted for standard acquisitions is as follows: a measuring tape is stretched out on the ground over a length of 86 m. Twenty-four 5 Hz-geophones are arranged with a spacing of $\Delta x = 2$ m from coordinate $x = 20$ m to coordinate $x = 66$ m (i.e., $L = 46$ m). In general, shots were hit in five positions: 20 m and 4 m from the first geophone (i.e., at coordinates $x = 0$ and 16 m), at the centre of the array (i.e., at $x = 43$ m), and at 4 and 20 m beyond the last geophone (i.e., at $x = 70$ and 86 m). These measurements are taken twice, once with 24 vertical geophones for Rayleigh wave recordings, and a second time with 24 horizontal geophones for Love wave recordings. In the first case, the ground is struck vertically with a 4 kg sledgehammer. In the second case, the ground is struck with this sledgehammer as horizontally as possible in holes previously dug in a V-shape. MASW was implemented as close to the accelerometer station as possible. An example of the MASW experimental line is shown in Fig. 4 for the ITS1 station.

We then applied a ‘FK-linear’ type processing to the data using Geopsy software (Wathelet et al. 2020), supplemented by tools developed in Matlab. FK processing is applied to each ‘sledgehammer shot’. The best shots are then selected, and a ‘stack’ is performed in the frequency domain (this approach allows for better preservation of high frequencies and objective selection of the best shots by visualizing the result of the FK processing for each of them).

Figure 5 (upper raw) shows the results obtained after stacking in the frequency domain for the MASW acquisition performed at station PLA1 (vertical polarity). The resolution limits of MASW are debated in the scientific community. The most “optimistic” allow the picking of the dispersion curves up to a wavelength equal to the length of the MASW measurement line (Foti et al., 2018). However, O’Neil, (2003) has shown that it is more prudent to limit the picking of the dispersion curves to 0.4 times the total length of the profile. Numerical simulations carried out by Riaño et al. (2024) tend to confirm O’Neil's, (2003) conclusions. In the present study, we adopted the latter, stricter criterion. Figure 5 (bottom raw) shows the portions of the dispersion curves that have been selected for the example site for further analysis.

3.2 Ambient Vibration Array (AVA) method

The AVA method complements the MASW method. It is a passive method that uses energy generated by anthropogenic or natural noise sources and generally allows for greater investigation depths. It involves positioning several sensors in various geometries (triangles, circles, etc.) to record ambient vibrations. More details about the AVA deployment and data analyses methods can be found in the literature (among others: Bard et al., 2010; Cornou et al., 2006; Wathelet et al., 2008; Di Giulio et al., 2012; Foti et al., 2018; Garofalo et al., 2016; Yong et al., 2013).

To carry out AVA measurements, we used 36 SmartSolo IGU-16HR 5 Hz three-component seismic nodes. Aswith MASW, the adopted deployment geometry is the one that has been proposed and successfully used to characterize stations in the French accelerometer network (Hollender et al. 2018). This approach includes the deployment of successive circular arrays; each composed of seven sensors distributed evenly around a central station. The radii of the circles increase progressively, with each new circle having a radius three times greater than that of the previous circle.

The nominal acquisition plan includes five circles with respective radii of 5 m (R1), 15 m (R2), 45 m (R3), 135 m (R4), and 405 m (R5). The objective is to enable simultaneous acquisition on at least two successive circles, such as R1 + R2, R2 + R3, etc. This requires the availability of at least 15 sensors, i.e., two circles of seven sensors each, plus the central sensor. For the field measurements of this study, we had enough sensors to deploy all 5 circles simultaneously.

The minimum acquisition times are as follows:

R1 + R2: 45 minutes

R2 + R3: 1 hour

R3 + R4: 2 hours

R4 + R5: 3 hours

This standard acquisition plan typically allows prospecting depths of 300 to 500 m to be reached. Obviously, the nominal geometry is subject to local accessibility constraints. However, the AVA method is “tolerant” to deviations from the perfect circular design geometry. Circles are often off-center to take access conditions into account, but also sometimes to keep all acquisition points on relatively homogeneous geology. For station SIA1, due to undesired restrictions in space, an L-shaped layout for AVA has been deployed in place of the two smaller circular arrays (R1 and R2). An example of the geometry of the AVA deployment is shown in Fig. 4 for the ITS1 station. The geometries of the deployments for all herein studied sites are given in the Online Resource (Figures ESM 1 to ESM 12).

The following systematic processing was applied to the AVA data:

“Classic” FK (McMechan and Yedlin 1981), applied to the vertical component only for the analysis of Rayleigh wave dispersion,

HRFK (or “high-resolution” FK) (Capon 1969), also applied to the vertical component only for the analysis of Rayleigh wave dispersion,

Transverse HRFK, applied to the horizontal components for the analysis of Love wave dispersion,

RTBF (Wathelet et al. 2018), which is a 3-component processing method that analyzes the entire ellipticity of Rayleigh waves, resulting in Rayleigh wave dispersion curves accompanied by an analysis of the polarity of the ellipticity, allowing for better mode identification.

These methods were applied to the following array sets: R1, R1R2, R2, R2R3, R3, R3R4, R4, R4R5, and R5 using the Geopsy software package. For efficiency, these processing were performed using command lines rather than the Geopsy graphical interface. Post-processing (visualization of results, semi-automatic scoring of scatter plots, etc.) was performed using in house Matlab scripts. It should be noted that we favored the FK-type processing and did not perform any SPAC-type processing.

Figure 6 shows example results obtained after processing ambient noise recordings by the FK, HRFK and RTBF methods for the PLA1 station site. The results of the RTBF processing are presented by differentiating between: (1) the dispersion curves obtained for negative ellipticities (RTBF-: retrograde Rayleigh wave particle motion), and (2) the dispersion curves obtained for positive ellipticities (RTBF+: prograde particle motion). As in MASW, before plotting the dispersion curves, it is important to calculate the array resolution limits, which depend on the acquisition geometry. The low-frequency resolution limit of an array is called λ_{max} (or k_{min}). For FK processing, it is advisable not to pick the dispersion curve below this value. For HRFK or RTBF processing, it is possible to pick up to a maximum wavelength of $2\lambda_{max}$ (or $k_{min}/2$) (Foti et al. 2018).

Figure 7 shows the results presented in Fig. 6 with a different color scale and adding the portions of dispersion curves that were picked. We prioritize the results obtained with RTBF processing: experience shows that these are generally the most reliable data.

Regarding the requirements for site characterization performed in this study - using MASW and/or AVA techniques - are required:2 vehicles, 48 geophones with a datalogger, 36 seismic nodes, and a team of 5 people to acquire sufficient data within a single day per site.

3.3 HVSR

We also applied the HVSR method to the sites studied. The HVSR method (Nakamura 1989, Bard 2008) is based on recording ambient vibrations measured on a single 3-component sensor. It consists of calculating the ratio of the Fourier spectra of the horizontal and vertical components. It allows the estimation of the fundamental resonance frequency of a site to be determined (f_0). The phenomenology explaining the existence of this peak is dominated by the frequency variation in the ellipticity of the ground motion associated with Rayleigh waves. The f_0 value is also often used in the final inversion process, where it complements the dispersion curves (joint inversion).

Figure 8 summarizes the HVSR results for the twelve characterized sites. In the frequency range 0.2–15 Hz, stations AIG2, ART2, ATH5, SEIS, SIA1, and VSK1 exhibit nearly flat HVSRs with amplitudes below 2. As expected from ambient vibration analyses, these stations show HVSR signatures typical of rock sites. For station SEIS, the mean HVSR curve exceeds 2 only at high frequencies (f_0> 15 Hz), and for SIA1 a similar increase is observed at even higher frequencies (f_0> 30 Hz). In contrast, stations ARG2, ITS1, JAN2, LEF2, LXR2, and PLA1 show distinct single or double peaks at both low (f_0< 1.0 Hz) and high (f_0> 2.0 Hz) frequencies, with corresponding amplitudes between 2.5 and 5, indicative of stiff to soft soil conditions.

It should be noted that the JAN2 site posed significant challenges for the noise analysis, with strong lateral variability observed among the AVA array stations. The site is highly urbanized, affected by multiple local noise sources (heavy traffic, pedestrian activity), as well as by the presence of underground structures, such as a nearby underground parking garage. The HVSR response at this site should therefore be interpreted with caution, particularly the large-amplitude peak between 0.8 and 1 Hz.

4 INVERSION AND RESULTS

4.1 Dispersion Curves and Inversion

Inversion consists of using the information contained in the dispersion curves (Rayleigh and/or Love waves), possibly supplemented by the site resonance frequency or the complete Rayleigh wave ellipticity curve, to calculate one or more S-wave velocity profiles compatible with this information. All other information available on the site that could help to better constrain the inversion is considered: geotechnical data providing orders of magnitude for soil stiffness, geological information providing, for example, the depth of the bedrock from a borehole or allowing its geological nature to be determined, etc. The depth of the bedrock, if it is known with certainty (e.g., from drilling), can be incorporated into the inversion.

The inversion process is iterative: the algorithm starts from an initial velocity model, directly calculates the resulting dispersion curves (and other possible parameters), and quantifies the difference (or "misfit") between the obtained dispersion curves and the experimental ones. The algorithm then modifies the initial velocity profile, performs a new direct calculation, a new estimation of the misfit, etc. The performance of the algorithm lies in its ability to modify the velocity profile to obtain a minimal misfit with a minimal number of iterations.

We performed the dispersion curves inversions using the Dinver tool (Wathelet 2008) from the Geopsy suite, which uses a neighborhood algorithm. The classic approach consists of searching for the profile for which the misfit is minimal: this is referred to as the best-estimate search. We applied this approach considering certain limitations. When inversion algorithms are set to search for a best-estimate solution, they often focus on a local minimum and ultimately produce a non-realistic profile. Furthermore, the production of a single velocity profile does not reflect the non-uniqueness of the inversion. Non-uniqueness implies that several velocity profiles can satisfy the same dispersion curve and its standard deviation, often with equally small misfits.

We therefore applied a slightly different approach that instead of inverting for a single, best-estimate profile, it inverts for a large number of profiles, often referred to as "acceptable misfit profiles" (Lomax and Snieder, 1995). This set of velocity profiles are linked to dispersion curves that remain "acceptable", i.e., within some user-defined level of the error bars of the measured dispersion curves. During the inversion process, several thousand "acceptable" profiles are retained.

Prior to the inversion step, all the picked dispersion curves (Rayleigh, Love, fundamental and possibly higher modes) are gathered. These different dispersion curves are then assembled (by site, wave type, and mode), merged, and possibly smoothed to obtain the widest possible dispersion curve per site. These dispersion curves, known as "targets" (or "target"), are established with their uncertainties and constitute the main input data for the inversion step.

The results of the inversion are illustrated in Fig. 9, using the ITS1 station as an example. The upper part of this figure shows the different "target" dispersion curves corresponding to the experimental measurements, including error bars. In the case of station ITS1, three Rayleigh modes were identified (the fundamental mode R0, and the first and second higher modes R1 and R2), as well as the fundamental Love mode (L0). The lighter shaded lines represent the forward-computed dispersion curves using the "acceptable velocity profiles" (several thousand) obtained by the inversion process. The center row of the figure shows these acceptable velocity profiles at different scales. This representation includes all the thousands of compatible profiles (in gray), as well as a subset of 33 randomly selected profiles whose distribution in V_{S30} is representative of that obtained for all the profiles resulting from the acceptable misfit approach (several thousand). Details of this random sampling of the numerous profiles to account for the variability are presented in Hollender et al. (2018). Finally, the lower row of this figure illustrates the distributions of V_{S30}, H_{800}, and the probabilities of the examined site to belong to any of the soil classes defined by EC8. The same representation is provided for all twelve characterized station sites in the Online Resource (Figures ESM 13 to ESM 24).

The 33 randomly chosen 1D $V_S(z)$ profiles for all the 12 examined station sites are summarized in Fig. 10 along with their average V_{S30} values. In all cases in this work, the V_{S30} value was computed from the ground surface down to a depth of 30 meters. This value characterizes an intrinsic property of the site (V_{S30}^{Site}). For stations installed below the surface, an additional V_{S30} value was computed from the installation depth ($z_{station}$) down to $z_{station}$+ 30 m. This parameter is referred to here as $V_{S30}^{Station}$.

In Table 3, a summary of the parameters extracted from the $V_S(z)$ profiles (V_{S30}^{Site}, $V_{S30}^{Station}$, H_{800} and EC8 soil category) is given. The proposed standard deviations were calculated assuming that the distributions are broadly normal, which is generally an acceptable assumption for the V_{S30} parameter. However, this assumption does not always hold true for the H_{800} parameter, whose determination is more sensitive to the choices made in the processing protocol, particularly the inversion settings. This behavior is particularly evident in the case of station ITS1 (see Fig. 9). We have therefore added a column in Table 3 providing a qualitative comment on the shape of the H_{800} distribution.

Table 3
Summary of selected parameters of site characterization for the twelve investigated HA

Station code	Station depth [m]	$\varvecV_{\varvecS30}^{\varvecS\varvecI\varvecT\varvecE}$ [m/s]	$\varvecV_{\varvecS30}^{\varvecS\varvecT\varvecA\varvecT\varvecI\varvecO\varvecN}$ [m/s]	$\varvecH_{800}^{\varvecS\varvec}$ [m]
AIG2	0	618 ± 27	618 ± 27	25 ± 9
ARG2	0	540 ± 36	540 ± 36	16 ± 19
ART2	0	1979 ± 74	1979 ± 74	1 ± 1
ATH5	3	855 ± 18	1149 ± 38	2 ± 0.3
ITS1	3	467 ± 11	548 ± 11	131 ± 49
JAN2	2	369 ± 13	402 ± 15	34 ± 17
LEF2	3	366 ± 10	380 ± 10	70 ± 152
LXR2	2	444 ± 9	489 ± 9	121 ± 11
PLA1	3	421 ± 6	485 ± 6	205 ± 123
SEIS	1.5	1049 ± 41	1395 ± 41	5 ± 1
SIA1	0	900 ± 22	900 ± 22	12 ± 4
VSK1	0	1359 ± 73	1359 ± 73	4 ± 2

In both Fig. 10 and Table 3, the site of station ART2 clearly stands out from the other station sites, with a $V_{S30}^{Station}$ reaching a value of almost 2000 m/s. Stations SEIS and VSK1 also show relatively high values of $V_{S30}^{Station}$, $i.e,$ between 1350 and 1400 m/s. The station with the lowest $V_{S30}^{Station}$ value is LEF2 (= 380 m/s).

In Fig. 11 we compare the measured V_{S30}^{Site} values for the twelve stations of the HAN in this study with the corresponding inferred values reported in Stewart et al. (2014) based on the surface geology and the topographic slope. Although the number of examined sites is limited, there is a significant deviation of the plotted points from the bisector. This suggests that the previously inferred V_{S30}^{Site} significantly underestimate the reality, especially for $V_{S30}^{Site} > 500$ m/s.

5 CONCLUSIONS

This study provides a homogeneous and detailed geophysical characterization of twelve accelerometric stations of the Hellenic Accelerometer Network (HAN), combining the active MASW and the passive AVA surface-wave methods. Apart from providing measured V_{S30} values and V_S profiles to complement the small tank of such information on permanent Greek accelerometric stations, the consistent application of the “acceptable misfit” inversion approach allows for the quantification of the epistemic uncertainty in the proposed profiles and related site parameters.

The results show that, for stiff soil and rock sites, geology- and slope-inferred V_{S30} values often underestimate the actual V_{S30}, in some cases markedly, especially for V_{S30} > 500 m/s. Only a few sites (ART2, SEIS, VSK1) exhibit genuinely hard-rock characteristics (V_{S30} > 1,000 m/s and H_{800} < 5 m). Station ART2, with a V_{S30} value close to 2000 m/s, clearly stands out as the most suitable candidate for a reference “rock” site in Greece, at least among the studied station sites.

The observed discrepancies between proxy-based indicators and in situ measurements highlight that indirect approaches alone may not always provide a sufficiently robust basis for site classification, particularly for critical applications such as reference rock-site selection. For stations intended to serve as references in GMMs or GITs frameworks, field measurements appear essential to ensure quantitative reliability and to avoid systematic bias.

These results emphasize the importance of direct geophysical investigations for reliable site classification and for reducing bias in Ground-Motion Models (GMMs) and Generalized Inversion Techniques (GITs). This new set of station site characterization metadata provides a reference framework for future updates of the HAN database and contributes to the harmonization of the European strong-motion station metadata within EPOS and ESM databases

(https://esm-db.eu). The results of this study have already been used in the derivation of a new Ground-Motion Model for very hard-rock conditions (Shible et al., 2026) as well as for investigating the impact of buildings on ground motion recordings, the so-called Soil-Structure Interaction-SSI (Rischette et al., 2026).

Declarations

Competitive Interests

The authors declare that they have no known competing financial or non-financial interests that could have appeared to influence the work reported in this paper.

Funding

This work was supported by the French Atomic and Alternative Energies Commission [CEA] and Electricité de France [EDF], within the framework of the CASHIMA3 and SIGMA3 research programs on seismic hazard assessment. SIGMA3 (2024–2028, www.sigma-programs.com) is funded by an industrial consortium composed of Electricité de France [EDF], French Atomic and Alternative Energies Commission [CEA], České energetické závody [Czech Energy Company, CEZ] Group, Pacific Gas and Electric Company [PG&E], VTT research center, SwissNuclear, Central Research Institute of the Electric Power Industry [CRIEPI], Stük, Uniper and Vattenfall. In addition, it was partially supported by the Earthquake Planning & Protection Organization's project "Updated Seismic Hazard Maps in the Area of Greece (2025, No. 12788)".

Authors Contributions

All authors contributed to data acquisition and data analysis used in this study. The overall structure and the main writing of the manuscript were carried out by N. Theodoulidis and F. Hollender. The latter significantly contributed and supervised the data analyses as well. All authors reviewed the manuscript, contributed to the revisions, and approved the final version.

Acknowledgements

The authors would like to thank Isabelle Douste-Bacqué, Margaux Buscetti, Harris Moustakas, Vasiliki Tsoukala and Maria-Georgia Dasoula for their help in acquiring the geophysical measurements, and for performing first stages of their treatment.

Data Availability

The datasets generated and/or analysed during the current study are available from the corresponding author upon reasonable request.

References

1. Bard P-Y (2008) Foreword: The H/V technique: capabilities and limitations based on the results of the SESAME project. Bull Earthq Eng 6:1–2. https://doi.org/10.1007/s10518-008-9059-4
2. Bard PY, Cadet H, Endrun B, Hobiger M, Renalier F, Theodulidis N, Ohrnberger M, Fäh D, Sabetta F, Teves-Costa P, Duval AM (2010) From non-invasive site characterization to site amplification: recent advances in the use of ambient vibration measurements. Earthq Eng Eur 105–123
3. Boore DM, Joyner WB (1997) Site Amplifications for Generic Rock Sites. Bull Seismol Soc Am 87:327–341
4. Borcherdt RD (1994) Estimates of Site-Dependent Response Spectra for Design (Methodology and Justification). Earthq Spectra 10:617–653
5. Capon J (1969) High resolution frequency-wavenumber spectrum analysis. Proceedings of the IEEE, 57, 1408–1418
6. CEN (2004) Eurocode 8: Design of structures for earthquake resistance-part 1: general rules, seismic actions, and rules for buildings. European Committee for Standardization, Brussels
7. Cornou C, Ohrnberger M, Boore DM, Kudo K, Bard P-Y (2006) Derivation of structural models from ambient vibration array recordings: Results from an international blind test. Proc. third Int. Symp. Eff. Surf. Geol. Seism. motion, Grenoble, Fr. 1127–1219
8. Cultrera G, Cornou C, Di Giulio G, Bard P-Y (2021) Indicators for site characterization at seismicstation: recommendation from a dedicated survey. Bull Earthq Eng. https://doi.org/10.1007/s10518-021-01136-7
9. Di Giulio G, Savvaidis A, Ohrnberger M, Wathelet M, Cornou C, Knapmeyer-Endrun B, Renalier F, Theodoulidis N, Bard P-Y (2012) Exploring the model space and ranking a best class of models in surface-wave dispersion inversion: application at European strong-motion sites. Geophysics 77:147–166
10. Foti S, Parolai S, Albarello D, Picozzi M (2011) Application of surface wave methods for seismic site characterization. Surv Geophys 32(6):777–825
11. Foti S, Hollender F, Garofalo F, Albarello D, Asten M, Bard P-Y, Comina C, Cornou C, Cox B, Di Giulio G, Forbriger T, Hayashi K, Lunedei E, Martin A, Mercerat D, Ohrnberger M, Poggi V, Renalier F, Sicilia D, Socco V (2018) Guidelines for the good practice of surface wave analysis: a product of the InterPACIFIC project. Bull Earthq Eng 16:2367–2420
12. Garofalo F, Foti S, Hollender F, Bard P-Y, Cornou C, Cox BR, Dechamp A, Ohrnberger M, Perron V, Sicilia D, Teague D, Vergniault C (2016) InterPACIFIC project: comparison of invasive and non-invasive methods for seismic site characterization. Part II: inter-comparison between surface-wave and

borehole methods. Soil Dynam Earthq Eng 82:241–254

13. Grendas I, Theodoulidis N, Hollender F, Hatzidimitriou P (2021) A GIT algorithm for simultaneous estimation of seismic source, site response and regional-distance dependent attenuation parameters: application to synthetic and real data. J Seismol. 1–24
14. Grendas I, Theodoulidis N, Hollender F, Hatzidimitriou P (2022) Spectral decomposition of S-waves in investigating regional dependent attenuation and improving site amplification factors: A case study in western Greece. Bull Earthq Eng 20:6441–6465. https://doi.org/10.1007/s10518-022-01459-z
15. Hollender F, Cornou C, Dechamp A, Oghalaei K, Renalier F, Maufroy E, Burnouf C, Thomassin S, Wathelet M, Bard P-Y, Boutin V, Desbordes C, Douste-Bacqué I, Foundotos L, Guyonnet-Benaize C, Perron V, Régnier J, Roullé A, Langlais M, Sicilia D (2018) Characterization of site conditions (soil class, V_{S30}, velocity profiles) for 33 stations from the French permanent accelerometric network (RAP) using surface-wave methods. Bull Earthq Eng 16:2337–2365. https://doi.org/10.1007/s10518-017-0135-5
16. Ktenidou O-J, Pikoulis E-V, Papageorgiou A, Gkika F, Liakopoulos S, Cekinmez Z, Savvaidis P, Fragouli K-E, Chalaris F, Evangelidis C (2026) The quest for reference stations at the National Observatory of Athens, Greece. Nat Hazards Earth Syst Sci 26:41–83. https://doi.org/10.5194/nhess-26-41-2026
17. Lanzano G, Luzi L, Cauzzi C, Bienkowski J, Bindi D, Clinton J, Cocco M, D'Amico M, Douglas J, Faenza L, Felicetta C, Gallovic F, Giardini D, Ktenidou O-J, Lauciani V, Manakou M, Maufroy E, Michelini A, Haluk O, Puglia R, Rupakhety R, Russo E, Shahvar M, Sleeman R, Theodoulidis N (2021) Assessing European Strong-Motion Data: an update on ORFEUS Coordinated Services, Seismol. Res Lett XX 1–17. 10.1785/0220200398
18. Lee J, Sibley E, Bayudanto A, Choi H, Park S, Noh M (2025) A shear-wave velocity of reference rock for nuclear power plant sites in South Korea. Seismol Res Lett 96:3584–3596. 10.1785/0220240425
19. Lomax A, Snieder R (1995) Identifying sets of acceptable solutions to non-linear, geophysical inverse problems which have complicated misfit functions. Nonlinear Process Geophys 2:222–227
20. Maragkakis I (2022) Site Amplification Factors in stations of the National Network of Accelerometers in Greece. Master Thesis, Sch. Geol. Aristotle Univ. Thessaloniki 130 pp
21. Margaris B, Kalogeras I, Papaioannou C, Savvaidis A, Theodoulidis N (2014) Evaluation of the national strong motion network in Greece: deployment, data processing and site characterization. Bull Earthq Eng 12:237–254
22. Margaris B, Scordilis EM, Stewart JP, Boore DM, Theodoulidis N, Kalogeras I, Melis NS, Skarlatoudis AA, Klimis N, Seyhan E (2021) Hellenic Strong-Motion Database with Uniformly Assigned Source and Site Metadata for the Period 1972–2015. Seismol. Res. Lett.
23. Margaris BN, Boore DM (1998) Determination of Δσ and κo from response spectra of large earthquakes in Greece. Bull Seismol Soc Am 88:170–182
24. McMechan GA, Yedlin MJ (1981) Analysis of dispersive waves by wave field transformation. Geophysics 46:869–874. 10.1190/1.1441225
25. Nakamura Y (1989) A method for dynamic characteristics estimation of subsurface using microtremor on the ground surface. Railw Tech Res Inst Q Rep 30:25–30
26. Nakano K, Matsushima S, Kawase H (2015) Statistical Properties of Strong Ground Motions from the Generalized Spectral Inversion of Data Observed by K-NET, KiK-net, and the JMA Shindokei Network in Japan. Bull Seismol Soc Am 105:2662–2680. https://doi.org/10.1785/0120140349
27. Nazarian S, Stokoe KH, Hudson WR (1983) Use of spectral analysis of surface waves meth-od for determination of moduli and thicknesses of pavement systems. Trans. Res. Rec. 930, Washi
28. O'Neil A (2003) Full-waveform reflectivity for modelling, inversion and appraisal of seismic surface wave dispersion in shallow site investigations. PhD, Univ. West. Aust. Sch. Earth Geogr. Sci
29. Papadopoulos G, Fikos I, Garcia-Jerez A, Theodoulidis N, Vargemezis G (2023) Combination of passive and active methods towards site characterization of accelerometer stations in Greece, NSGeophys, 1–21, doi.org.10.1002/nsg.12248
30. Park CB, Miller RD, Xia J (1998) Ground roll as a tool to image near-surface anomaly. SEG Tech. Progr. Expand. Abstr. 1998 874–877, Society of Exploration Geophysicists
31. Park CB, Miller RD, Xia J (1999) Multichannel analysis of surface waves. Geophysics 64(3):800–808. https://doi.org/10.1190/1.1444590
32. Pilz M, Cotton F, Kotha SR (2020) Data driven and machine learning identification of seismic reference stations in Europe. Geophys J Int 222:861–873
33. Riaño AC, Lopez-Caballero F, Hollender F (2024) Evaluating and validating 3-D simulated MASW and SPAC in situ tests in Argostoli, Greece. Geophys J Int 238:1053–1072. https://doi.org/10.1093/gji/ggae187
34. Richart FE, Hall JR, Woods RD (1970) Vibrations of soils and foundations. Prentice-Hall, Inc., Englewood Cliffs, N. Jersey, p 414
35. Rischette P, Theodoulidis N, Hollender F, Perron V, Traversa P, Roumelioti Z, Bard P-Y, Buscetti M, Douste-Bacqué I (2026) Impact of building on ground motion recordings: Insights from nine permanent accelerometric stations in Greece. Bull Earthq Eng (submitted for publication).
36. Shible H, Hollender F, Bindi D, Traversa P, Oth A, Edwards B, Klin P, Kawase H, Grendas I, Castro RR, Theodoulidis N, Gueguen P (2022) GITEC: A Generalized Inversion Technique Benchmark. Bull Seismol Soc Am 112:850–877. https://doi.org/10.1785/0120210242
37. Shible H, Hollender F, Traversa P, Bard P-Y (2023a) Ground-Motion Model for Hard-Rock Sites by Correction of Surface Recordings (Part 1): Comparison of Site-Response Estimates at KiK-Net Sites. Bull Seismol Soc Am. https://doi.org/10.1785/0120220203
38. Shible H, Traversa P, Hollender F, Bard P-Y (2023b) Ground-Motion Model for Hard-Rock Sites by Correction of Surface Recordings (Part 2): Correction, Mixed-Effects Regressions, and Results. Bull Seism Soc Am. https://doi.org/10.1785/0120220204
39. Shible H, Hollender F, Traversa P, Baumont D, Ameri G, Theodoulidis N (2026) Ground motion model for reference hard rock conditions in the Euro-Mediterranean context by GIT-based site response deconvolution. Bull. Seism. Soc. Am. (accepted
40. Steidl JH, Tumarkin AG, Archuleta RJ (1996) What is a reference? Bull. Seismol Soc Am 86:1743–1748

41. Stewart JP, Klimis N, Savvaidis A, Theodoulidis N, Zargli E, Athanasopoulos G, Pelekis P, Mylonakis G, Margaris B (2014) Compilation of a local Vs profile database and its application for inference of Vs30 from geologic- and terrain-based proxies. Bull Seismol Soc Am 104:2827–2841
42. Stokoe KH, Wright GW, James AB, Jose MR (1994) Characterization of geotechnical sites by SASW method. Geophys Charact sites 15–25
43. Theodoulidis N, Papazachos B (1992) Dependence of strong ground motion on magnitude-distance, site geology and macroseismic intensity for shallow earthquakes in Greece: I, Peak horizontal acceleration, velocity and displacement. Soil Dyn Earth Eng 11:387–402
44. Theodoulidis N, Maragakis I, Grendas I, Hatzidimitriou P, Kawase H, Ito E, Triantafyllidis P (2022) Estimation of S-wave Horizontal Spectral Amplification Factor(HSAF) from earthquake Horizontal-to-Vertical Spectral ratio(eHVSR) in Greece. 3rd Eur. Conf. Earthq. Eng. Seismol
45. Theodoulidis N, Margaris B, Papastamatiou D (1986) Accelerometers Network Planning in Greece (in Greek). Rep. ITSAK 86–04
46. Van Houtte C, Ktenidou OJ, Larkin T, Kaiser A (2012) Reference stations for Christchurch. Bull N Z Soc Earthq Engin 45(4):184–195
47. Wald D, Allen T (2007) Topographic slope as a proxy for seismic site conditions and amplification. Bull Seism Soc Am 97:1379–1395
48. Wathelet M (2008) An improved neighborhood algorithm: Parameter conditions and dynamic scaling. Geophys Res Lett 35. https://doi.org/10.1029/2008GL033256
49. Wathelet M, Jongmans D, Ohrnberger M, Bonnefoy-Claudet S (2008) Geopsy: A User-Friendly Open-Source Tool Set for Ambient Vibration Processing. Seismol Res Lett 91:1878–1889
50. Wathelet M, Guillier B, Roux P, Cornou C, Ohrnberger M (2018) Rayleigh wave three-component beamforming: signed ellipticity assessment from high-resolution frequency-wavenumber processing of ambient vibration arrays. Geophysl J Intern 215(1):507–523. https://doi.org/10.1093/gji/ggy286
51. Wathelet M, Chatelain J-L, Cornou C, Di Giulio G, Guillier B, Ohrnberger M, Savvaidis A (2020) Geopsy: A User-Friendly Open-Source Tool Set for Ambient Vibration Processing. Seismol Res Lett 91:1878–1889. https://doi.org/10.1785/0220190360
52. Yong A, Martin A, Stokoe K, Diehl J (2013) ARRA-funded Vs30 measurements using multi-technique approach at strong-motion stations in California and central-eastern United States. U.S.G.S. Open-File Rep
53. Yong A, Askan A, Cassidy J, D'Amico M, Parolai S, Pilz M, Stephenson W (2022) Introduction to the special issue of the Consortium of Organizations for Strong Motion Observation Systems (COSMOS) international guidelines for applying noninvasive geophysical techniques to characterize seismic site conditions. J Seismol 26:557–566. https://doi.org/10.1007/s10950-022-10104-w

Figures

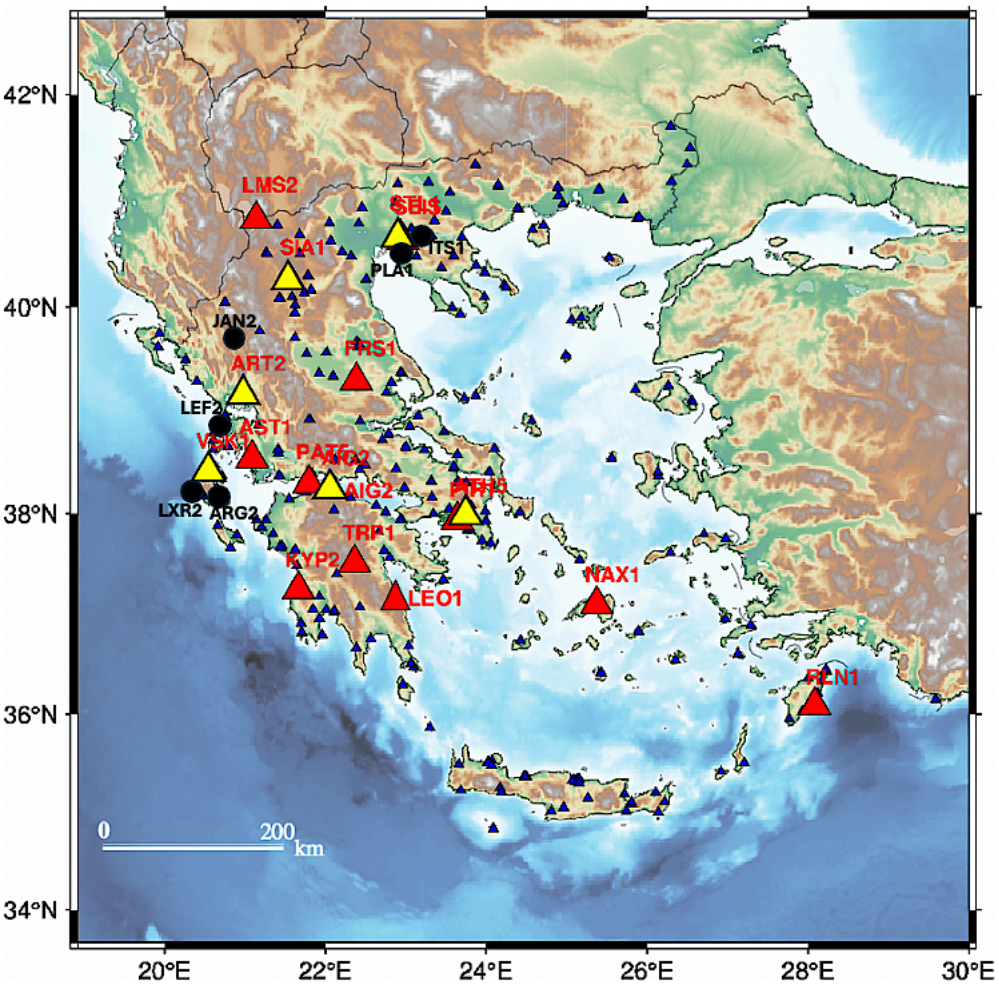


Figure 1

Accelerometer stations of the Hellenic Accelerometer Network (blue triangles) and the 17geologic “rock” stations selected after applying the criteria of Table 1 (red & yellow triangles). Sites characterized in the present study correspond to yellow triangles and 6 additional stiff-to-soft soil stations (black circles).

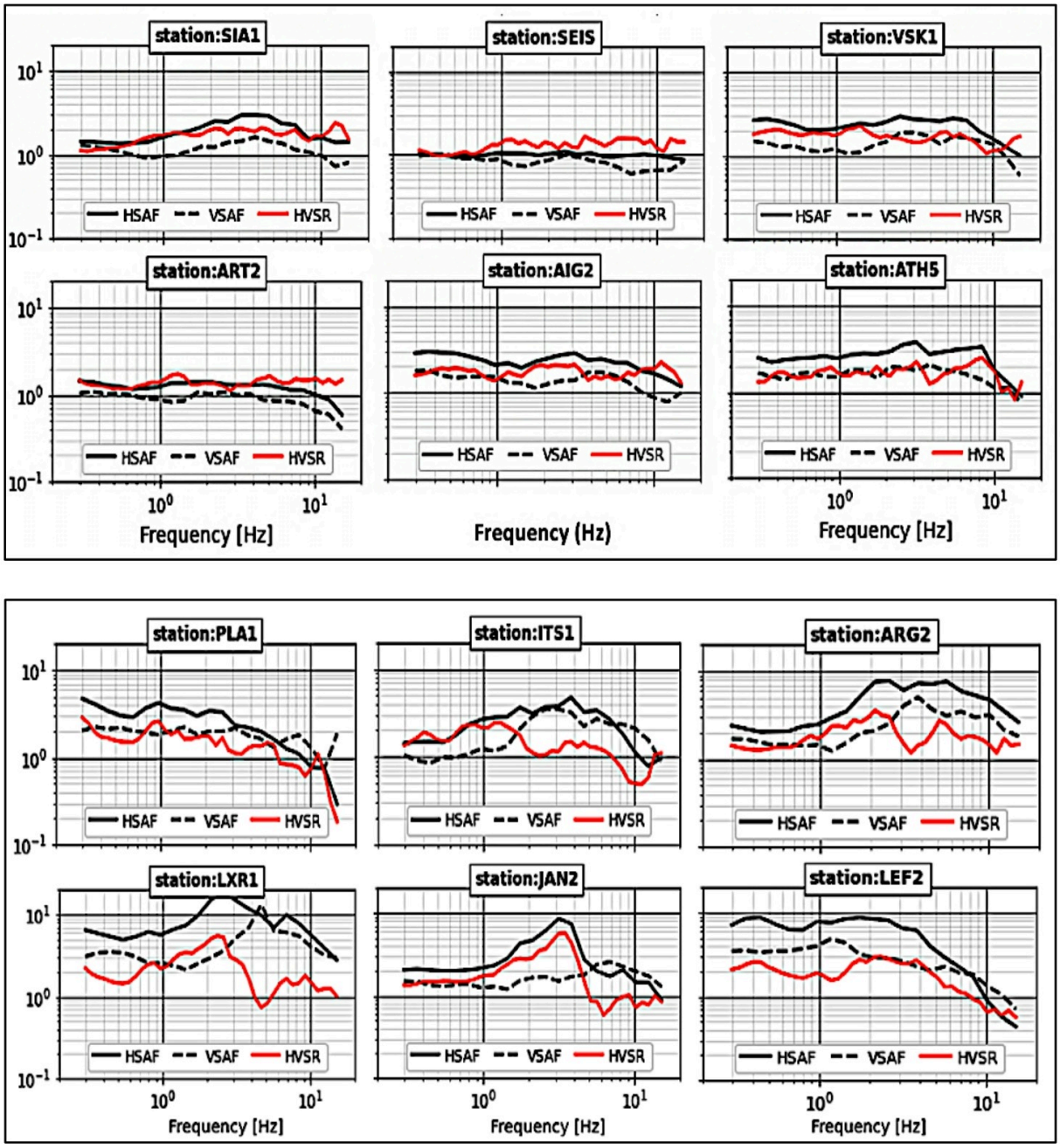


Figure 2

Horizonal Spectral Amplification Factors (black line) and Horizontal-to-Vertical Spectral Ratios (red line) for the 12 studied stations (after Maragakis, 2022).



Figure 3

Surface geology around the 12 studied sites. Geologic formations are grouped in five (5) categories according to their geologic age, based on maps in scale 1:50.000 (https://www.eagme.gr/). H: Holocene, PL: Pleistocene, Q: Quaternary undivided, T: Tertiary, MP: Mesozoic & Paleozoic (Stewart et al. 2014).

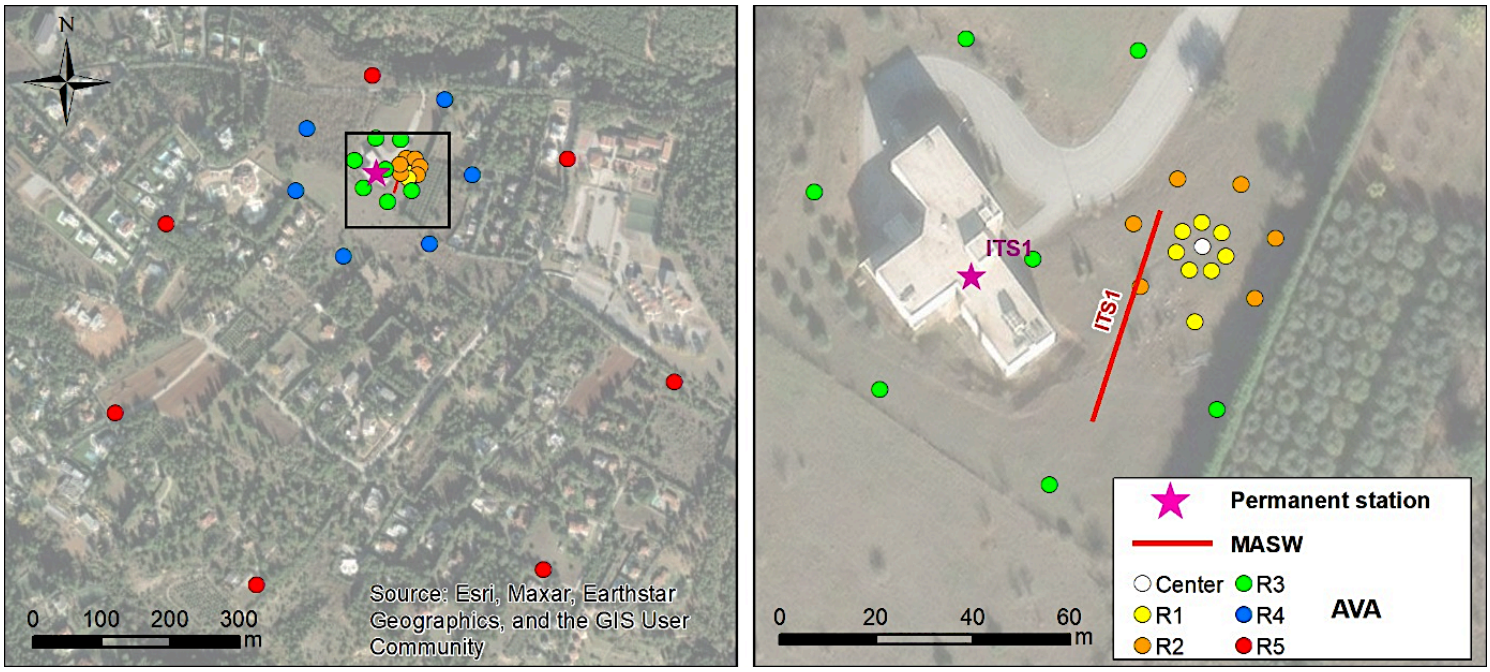


Figure 4

Configuration of MASW (red line) and AVA deployments (colored circles) for the ITS1 station site (left: overview; the area in the square is shown in close view to the right).

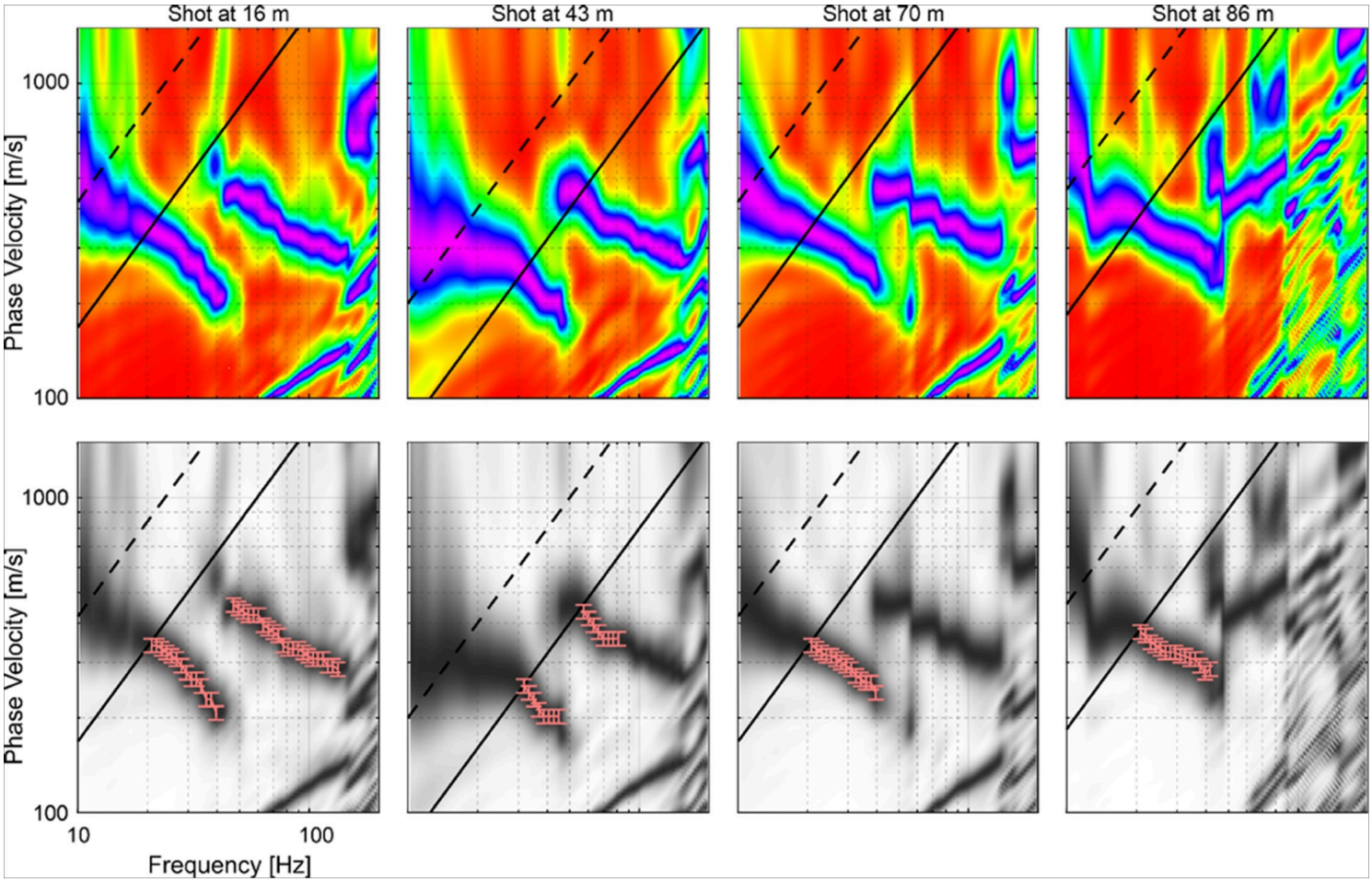


Figure 5

Dispersion curves for shots at various distances in color (top panels) and in grayscale (bottom panels). The latter include the picking (pink symbols) of the average phase velocities ± 1s.d. per frequency. Dashed and solid black lines mark the theoretical array resolution, i.e., the largest wavenumber resolved (kmin) and kmin/2, respectively. Our study adopts the stricter boundary, i.e., we usually pick phase velocities up to kmin/2. Results correspond to the PLA1 station site.

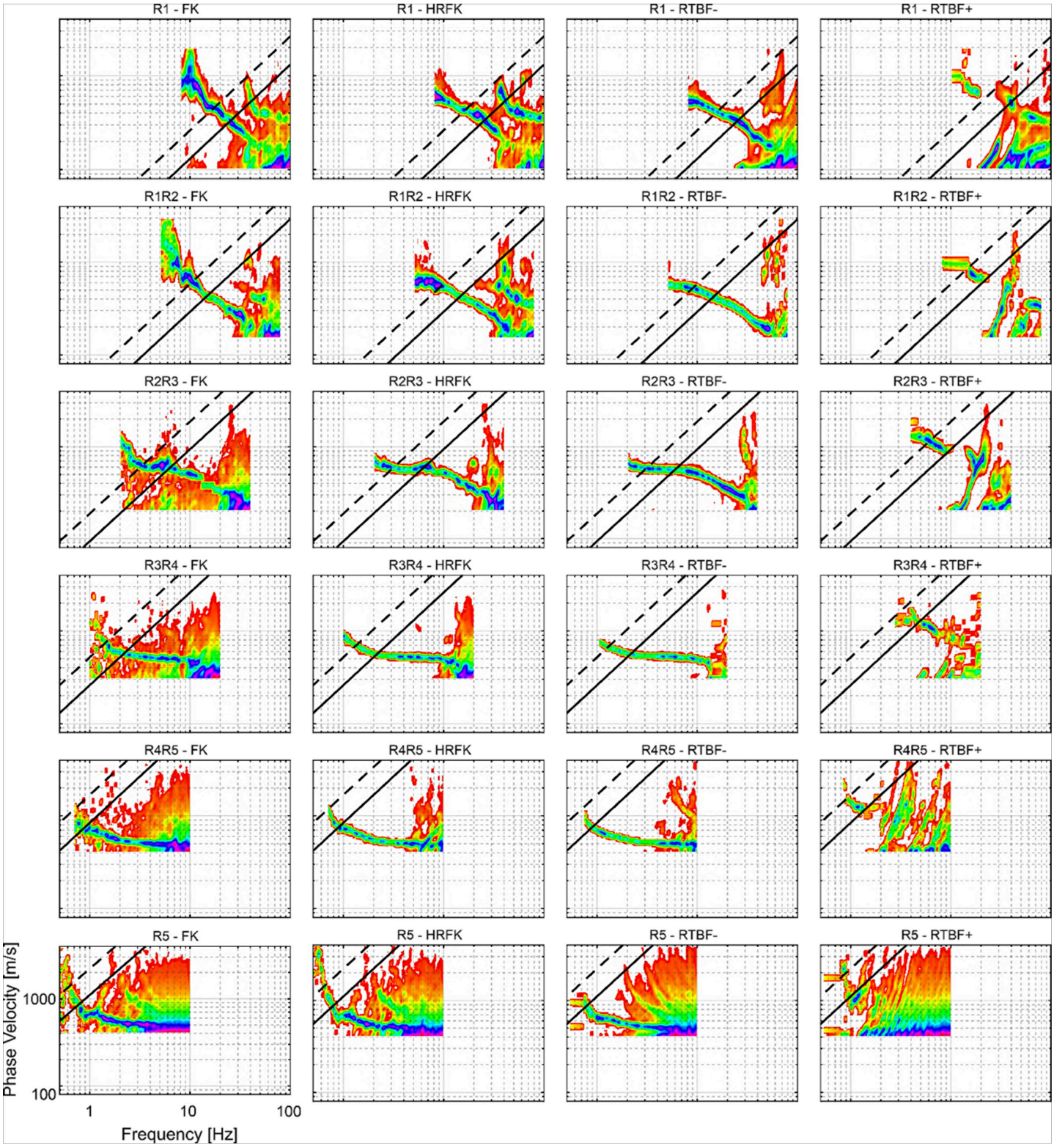


Figure 6

Dispersion Curves for various apertures of the AVA, using different processing techniques (from left to right column: FK, HRFK, RTBF^{-}, RTBF^{+}; see text for details). Example results correspond to the PLA1 station site.

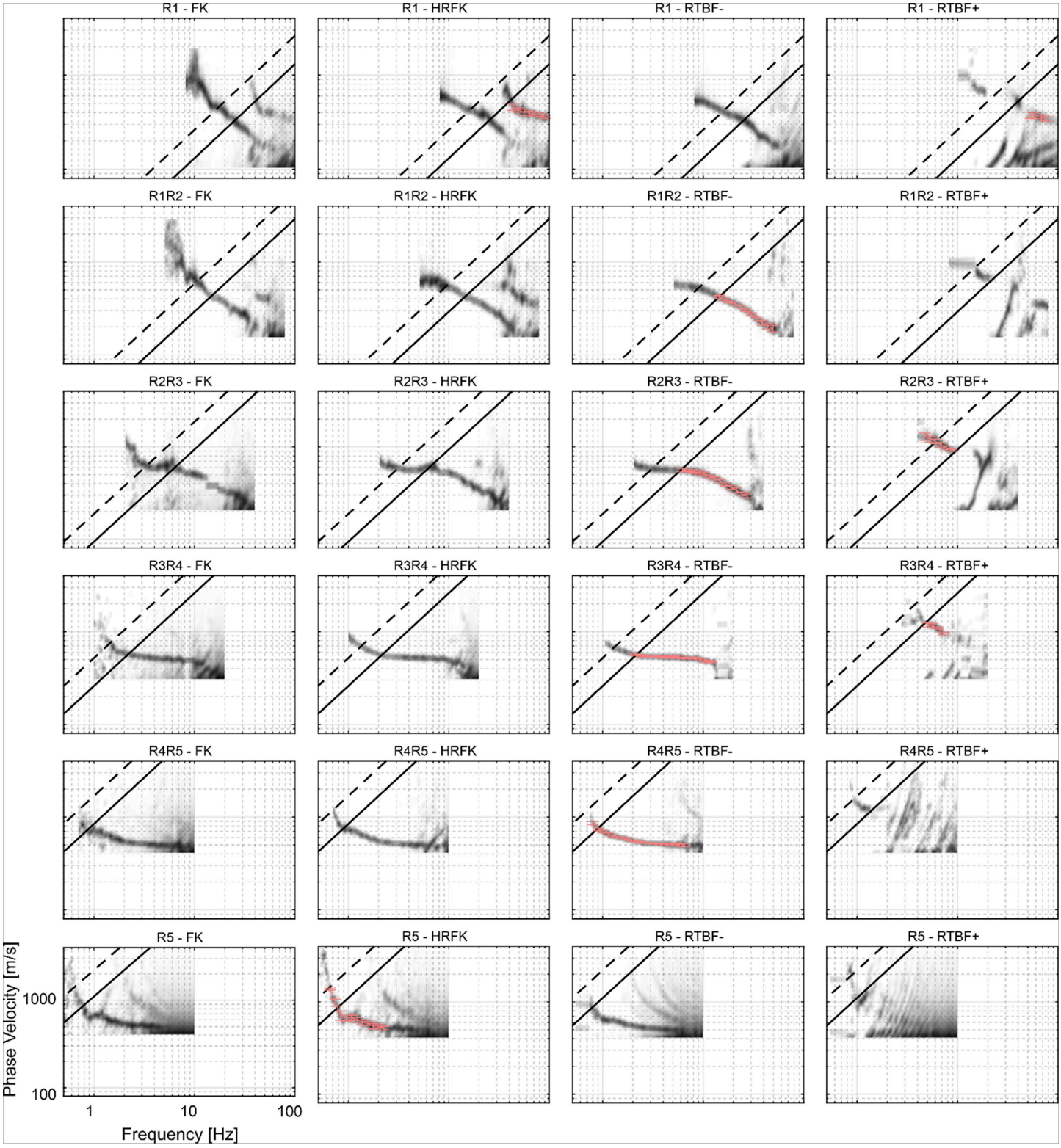


Figure 7

As in Figure 7 but in grayscale and with the addition of symbols to demonstrate the manually picked parts of the dispersion curves at PLA1.

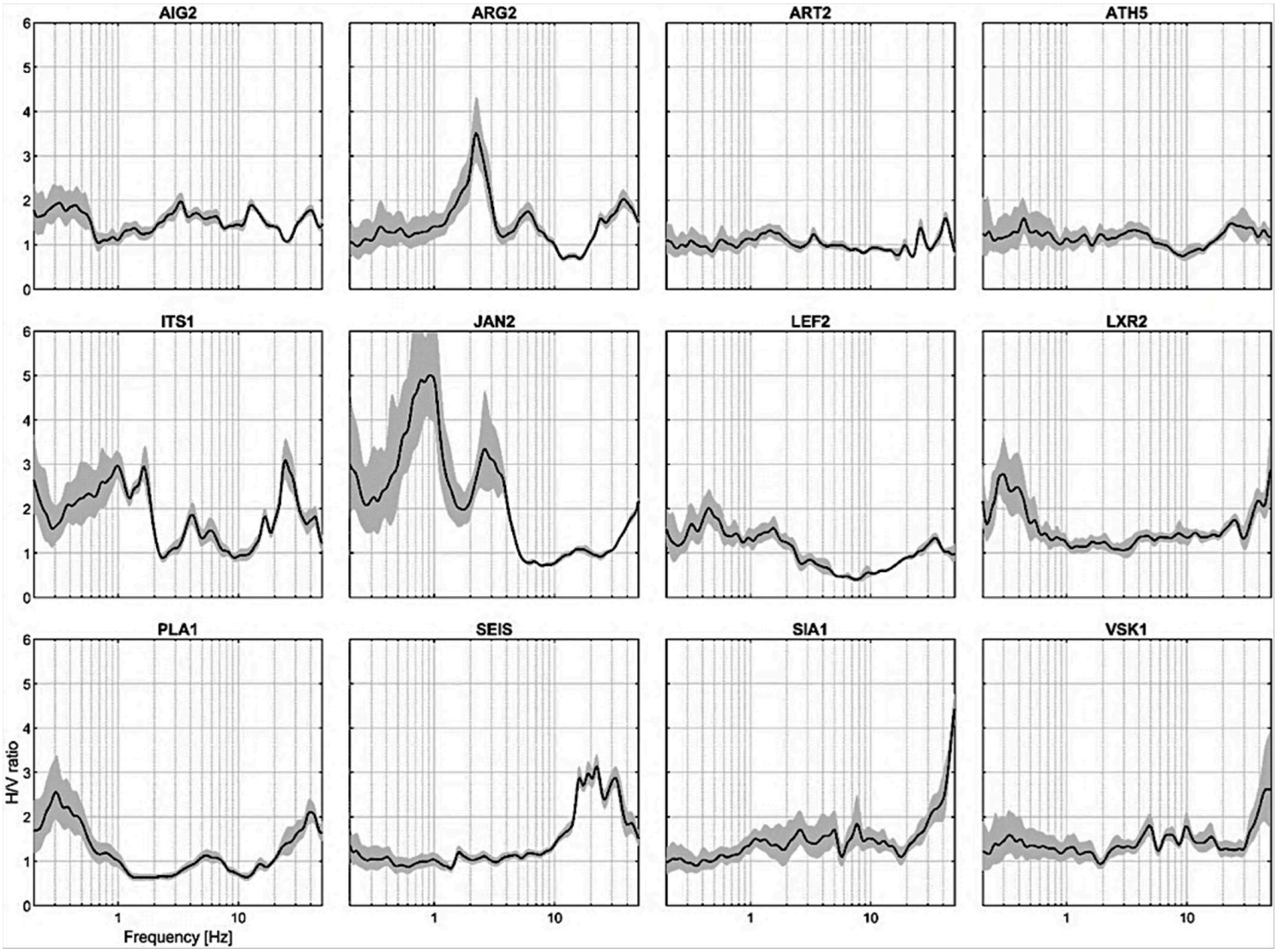


Figure 8

Experimental HVSRs for all investigated stations (solid line) ±1sd.

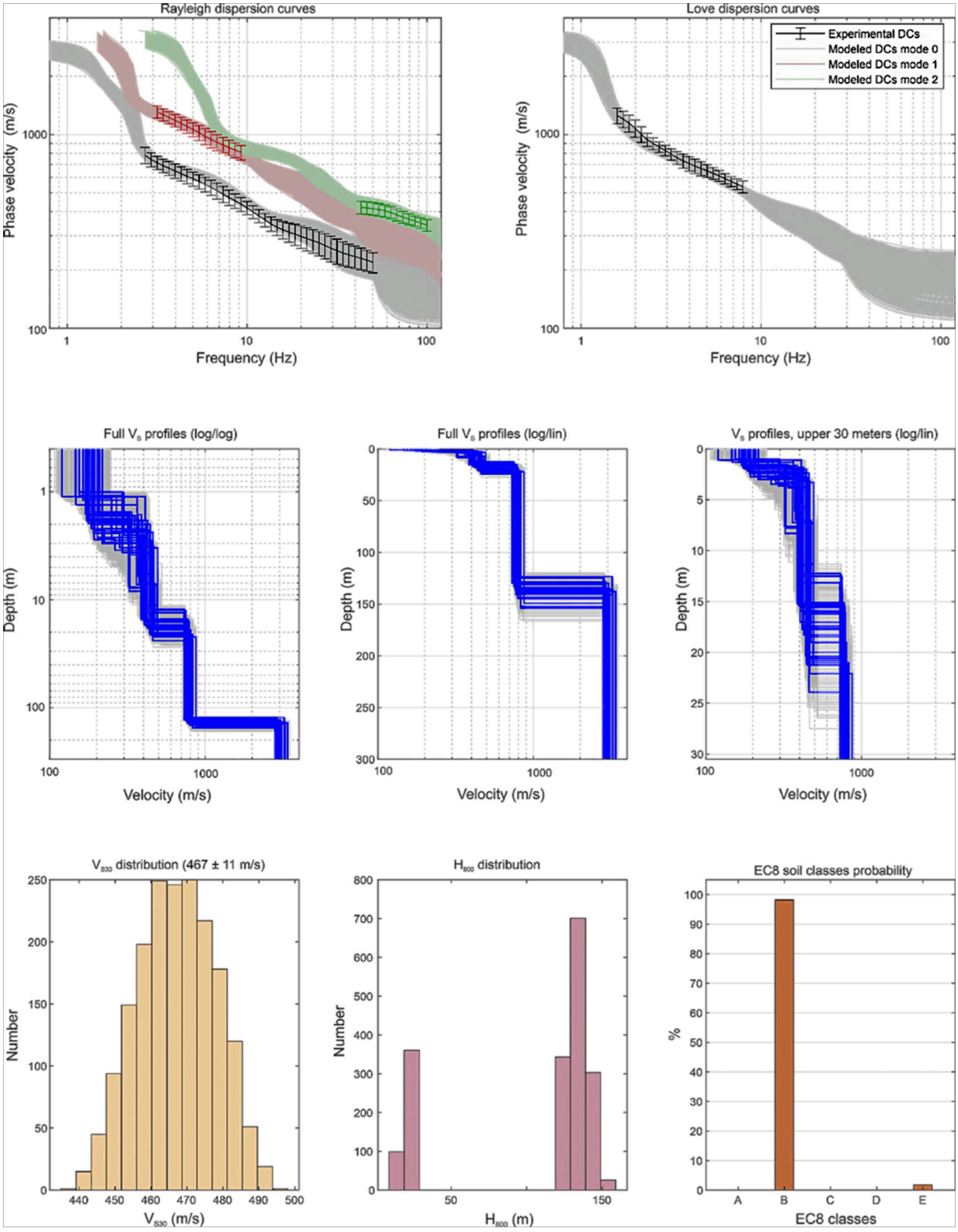


Figure 9

Inversion results for station ITS1 using the “Acceptable Misfit” approach, which consists of estimating many profiles compatible with the experimental data to estimate the uncertainty of the results. Top row: measured empirical dispersion curves and associated error bars; in light shades: ‘direct’ dispersion curves recalculated from the inverted profiles. Middle: in gray, inverted velocity profiles (several thousand); in blue, random selection of 33 profiles sampling the uncertainty. Bottom, from left to right: distribution of V_{S30} values (calculated on all velocity profiles of “acceptable misfit”); distribution of H_{800} values; probability of compliance with soil classes A to E of Eurocode 8 (calculated on all velocity profiles).

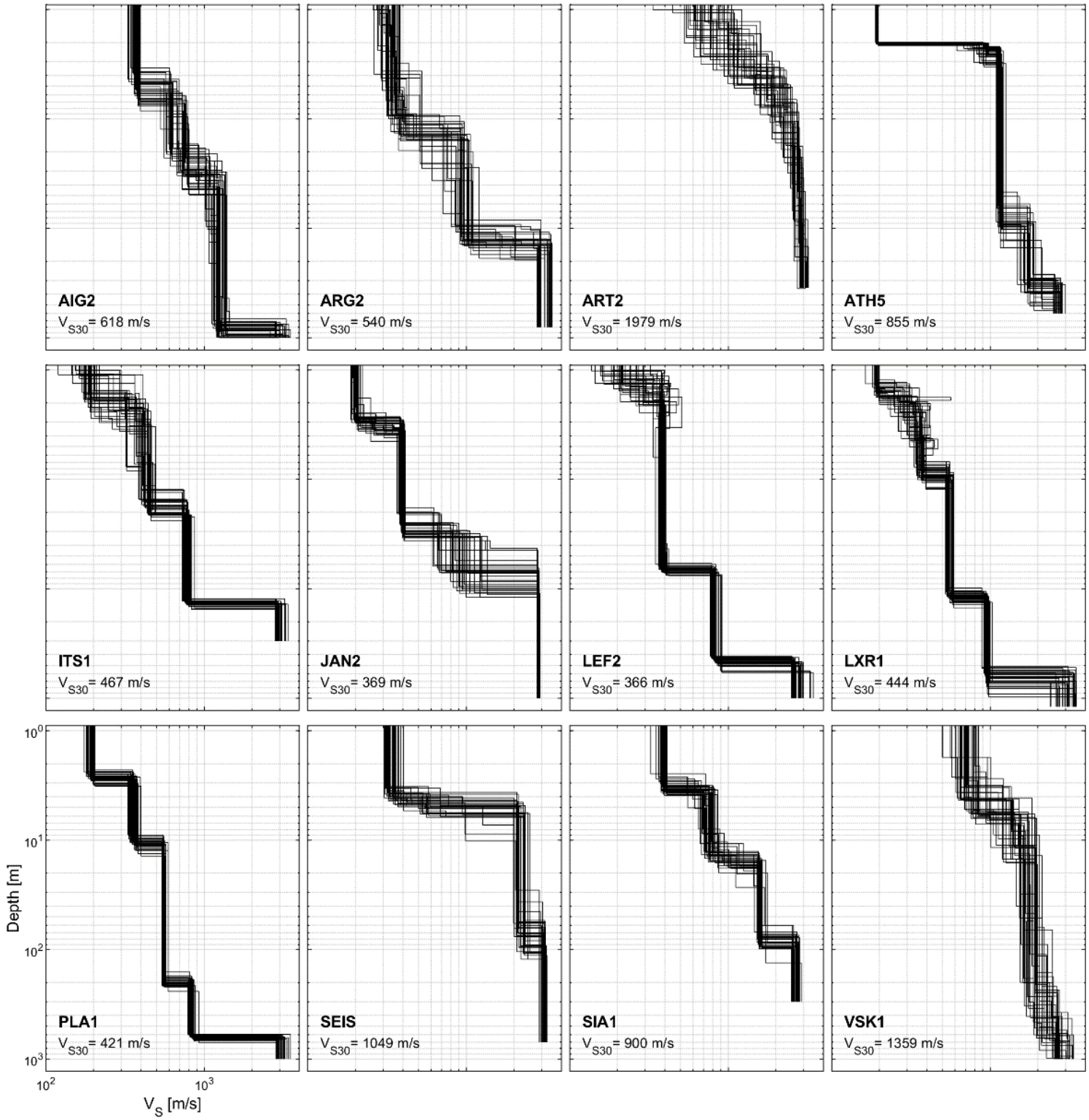


Figure 10

33 selected 1D V_S (z) profiles per station for all 12 investigated sites and their estimated V_{S30} values.

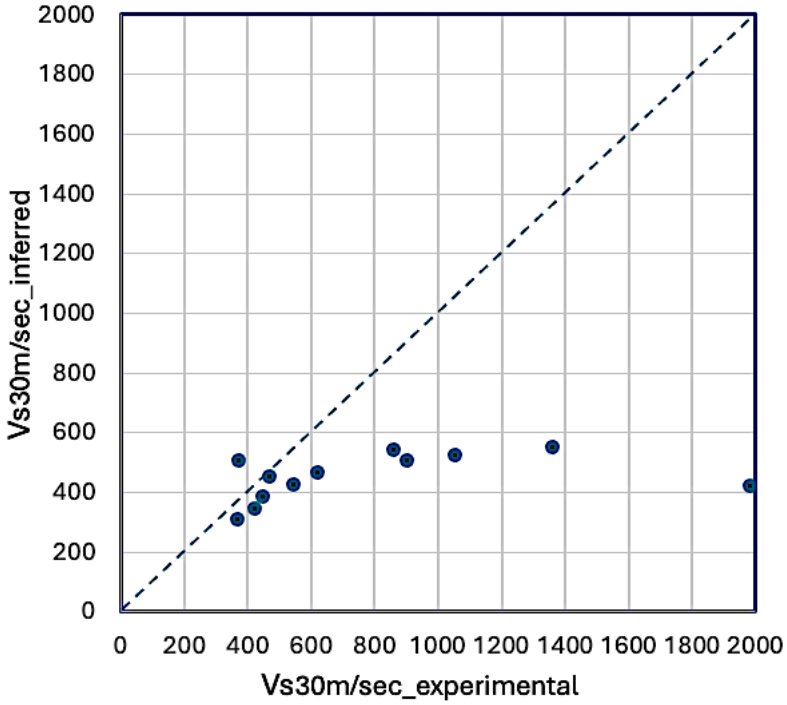


Figure 11

Comparison of the experimentally estimated V_{S30} values in this study with those previously inferred based on geology and topographic slope (Stewart et al. 2014).

Supplementary Files

This is a list of supplementary files associated with this preprint. Click to download.

- ELECTRONICSUPPLEMENT.docx